Electronic Supplementary Material (ESI) for Catalysis Science & Technology.

Electrocatalytic dimeric inactivation mechanism by porphyrinic molecular-type catalyst: integration in a glucose/O_2 Fuel Cell

Kamal Elouarzaki,[1,2] Vishvak Kannan, [2,3] Yian Wang,[2,4] Adrian C. Fisher*[2,4] and Jong-Min Lee* [1, 2]

[1] School of Chemical and Biomedical Engineering, Nanyang Technological University, 62 Nanyang Drive, Singapore 637459, Singapore
[2] Cambridge CARES, CREATE Tower, 1 CREATE Way, Singapore 138602, Singapore
[3] Department of Chemical and Biomolecular Engineering, National University of Singapore, Singapore
[4] Department of Chemical Engineering and Biotechnology, University of Cambridge, West Cambridge Site, Philippa Fawcett Drive, Cambridge CB3 0AS, United Kingdom

Characterization of the rhodium complex

NMR spectra were recorded on a Bruker AVANCE 400 operating at 400.0 MHz for ^{1}H. ESI mass spectra were recorded with a Bruker APEX-Qe ESI FT-ICR mass spectrometer. UV-visible spectra were recorded with a carry 1 spectrophotometer with a quartz cuvette (1 cm depth).

Deuteroporphyrine IX dimethyl ester Rhodium(III) (**(DPDE)Rh^{III}**) was characterized by electrospray ionisation mass spectrometry (ESI-MS), UV-visible spectroscopy (complete metallation was checked by disappearance of the Q band) and ^{1}H NMR :

^{1}H NMR ($CDCl_3$): δ 10-10.15 (3s, 4H), 9.1 (s, 2H), 4.28 (t, 4H), 3.7 (s, 6H), 3.6 (s, 6H), 3.52 (s, 6H), 3.15 (t, 4H).

UV-vis ($CHCl_3$) λ_{max}/nm ($mM^{-1}\,cm^{-1}$): 401 (127), 516 (16.3), 548 (24.6).

ESI-MS *m*/*z* (in ethanol): 639.0 $[(DPDE)Rh^{III}]^+$, 667.0 $[(DPDE)Rh^{III})(CO)]^+$.

Supplementary Tables

Supplementary Table 1: List of symbols and nomenclature

Roman		
A	electroactive surface area	cm^2
D_s	diffusion coefficient of substrate	$cm^2\,s^{-1}$
E	applied electrode potential	V
E_i	initial potential	V
E_j^0	standard potential of species j	V
E^{red}	reduction current peak potential	V
E^{ox}	oxidation current peak potential	V

ΔE^0	difference between standard potential of two species	V
F	Faraday constant	$C\ mol^{-1}$
I_j	current of species j	mA
k	second order rate constant for catalytic reaction	$cm^3\ s^{-1}\ mol^{-1}$
k_b	homogeneous rate constant for "backward" reaction	s^{-1}
k_f	homogeneous rate constant for "forward" reaction	s^{-1}
k_0^j	standard heterogeneous rate constant of species j	s^{-1}
k_{red}^j	heterogeneous rate constant for reduction of species j	s^{-1}
k_{ox}^j	heterogeneous rate constant for oxidation of species j	s^{-1}
K_A	equilibrium constant	–
$[P]$	product concentration	$mol\ cm^{-3}$
R	universal gas constant	$J\ mol^{-1}\ K^{-1}$
$[S]$	substrate concentration	$mol\ cm^{-3}$
$[S]^*$	substrate bulk concentration	$mol\ cm^{-3}$
t	time	s
T	absolute temperature	K
v	scan rate	$mV\ s^{-1}$
x	distance from the planar electrode	cm
Greek		
α	charge transfer coefficient	–
Γ_j	surface excess of species j	$mol\ cm^{-2}$
Γ^*	total surface excess	$mol\ cm^{-2}$

Supplementary Table 2: Summary of the parameters estimated from experiments employed for the numerical analyses of dimeric rhodium formation

Parameter	Value	Unit
A	1.0 ± 0.2	cm^2
E_i	-1.5	V
E_1^0	-0.475 ± 0.01	V
E_2^0	-0.475 ± 0.01	V
E_3^0	-0.475 ± 0.01	V
E_4^0	-1.36	V
E_v	0.2	V
F	96485	$C\,mol^{-1}$
k	$(1 \pm 0.1) \times 10^5$	$cm^3\,s^{-1}\,mol^{-1}$
k_{2f}	10^8	$cm^3\,s^{-1}\,mol^{-1}$
k_{2b}	≤ 1.0	s^{-1}
k_0^1	6.0	s^{-1}
k_0^2	3.5	s^{-1}
k_0^3	6.0	s^{-1}
k_0^4	10.0	s^{-1}
K_A	10^7	–
R	8.3145	$J\,mol^{-1}\,K^{-1}$
T	293.15	K
α	0.5	–

Γ^*	$(6 \pm 1) \times 10^{-10}$	$mol\ cm^{-2}$

Supplementary Table 3: Relative error between the model lacking dimer formation and experimental data at different scan rates

Scan rate (mV/s)	i_{pa} **(A)**	i_{pc} **(A)**	**Relative error**
5	0.1145	-0.089	22%
20	0.40744	-0.3485	14%
50	0.98156	-0.8785	10%
75	1.4159	-1.301	8%
100	1.8147	-1.681	7%
150	2.9401	-2.796	5%
200	3.9634	-3.745	6%
500	8.5304	-8.159	4%

Supplementary Methods

Supplementary methods 1:

The overall EC'CECE mechanism is summarised by Equations 1 to 6,

$$(DPDE)\mathrm{Rh^{III}} + \mathrm{e^-} \underset{k_{ox}^1}{\overset{k_{red}^1}{\rightleftharpoons}} (DPDE)\mathrm{Rh^{II}} + \mathrm{e^-} \underset{k_{ox}^2}{\overset{k_{red}^2}{\rightleftharpoons}} (DPDE)\mathrm{Rh^{I}} \quad (1)$$

$$(DPDE)Rh^{III} + [S] \overset{k}{\rightarrow} (DPDE)\mathrm{Rh^{I}} + [P] \quad (2)$$

$$(DPDE)Rh^{III} + \mathrm{OH^-} \underset{k_{1b}}{\overset{k_{1f}}{\rightleftharpoons}} (DPDE)Rh^{III}(OH) \quad (3)$$

$$(DPDE)Rh^{III}(OH) + \mathrm{e^-} \underset{k_{ox}^3}{\overset{k_{red}^3}{\rightleftharpoons}} (DPDE)\mathrm{Rh^{II}} + OH^- + \mathrm{e^-} \underset{k_{ox}^2}{\overset{k_{red}^2}{\rightleftharpoons}} (DPDE)\mathrm{Rh^{I}} + OH \quad (4)$$

$$2(DPDE)\mathrm{Rh^{II}} \underset{k_{2b}}{\overset{k_{2f}}{\rightleftharpoons}} \left[(DPDE)\mathrm{Rh^{II}}\right]_2 \quad (5)$$

$$\left[(DPDE)\mathrm{Rh^{II}}\right]_2 + 2\mathrm{e^-} \underset{k_{ox}^4}{\overset{k_{red}^4}{\rightleftharpoons}} 2(DPDE)\mathrm{Rh^{I}} \quad (6)$$

k_{red}^j and k_{ox}^j are the rate constants for jth step of electrochemical reactions, and k, k_{1f}, k_{1b}, k_{2f} and k_{2b} are the rate constants of the chemical reactions. The surface reaction is suggested to follow a semi-empirical Butler-Volmer (BV) equation for electron transfer and the diffusion of glucose obeys Fick's law in the solution. The validity of the scheme was evaluated by mathematical models. The equations for the model used in the EC'CECE simulations are derived as follows:

The governing equations for the surface concentrations of the rhodium species are:

$$\frac{\partial \Gamma_{Rh^I}}{\partial t} = -\frac{i_{Rh^{II}/Rh^I}}{FA} + k[S]\Gamma_{Rh^{III}} - \frac{1}{2}\frac{i_{\left[\mathrm{Rh^{II}}\right]_2/Rh^I}}{FA} \quad (7)$$

$$\frac{\partial \Gamma_{Rh^{II}}}{\partial t} = -\frac{i_{Rh^{III}/Rh^{II}}}{FA} - \frac{i_{Rh^{III}(OH)/Rh^{II}}}{FA} + \frac{i_{Rh^{II}/Rh^I}}{FA} + \frac{1}{2}k_{2b}\Gamma_{\left[\mathrm{Rh^{II}}\right]_2} - \frac{1}{2}k_{2f}\Gamma_{Rh^{II}}^2 \quad (8)$$

$$\frac{\partial \Gamma_{Rh^{III}}}{dt} = \frac{i_{Rh^{III}/Rh^{II}}}{FA} - k[S]\Gamma_{Rh^{III}} - k_f \Gamma_{Rh^{III}} + k_b \Gamma_{Rh^{III}(OH)} \tag{9}$$

$$\frac{\partial \Gamma_{Rh^{III}(OH)}}{\partial t} = k_f \Gamma_{Rh^{III}} - k_b \Gamma_{Rh^{III}(OH)} + \frac{i_{Rh^{III}(OH)/Rh^{II}}}{FA} \tag{10}$$

$$\frac{\partial \Gamma_{\left[\mathrm{Rh^{II}}\right]_2}}{\partial t} = \frac{i_{\left[\mathrm{Rh^{II}}\right]_2/Rh^{I}}}{FA} + k_{2f} \Gamma^{\,2}_{Rh^{II}} - k_{2b} \Gamma_{\left[\mathrm{Rh^{II}}\right]_2} \tag{11}$$

The overall surface concentration is a constant value and can be written as

$$\Gamma_{Rh^{I}} + \Gamma_{Rh^{II}} + \Gamma_{Rh^{III}} + \Gamma_{Rh^{III}(OH)} + \Gamma_{\left[\mathrm{Rh^{II}}\right]_2} = \Gamma^{*} \tag{12}$$

Substrate transport to the electrode surface is treated as a linear diffusion, and the equation is given

$$\frac{\partial [S]}{\partial t} = D_s \frac{\partial^2 [S]}{\partial x^2} - k[S]\Gamma_{Rh^{III}} \tag{13}$$

The contributions to the measured current are given from $i_{Rh^{II}/Rh^{I}}$, $i_{Rh^{III}/Rh^{II}}$, $i_{Rh^{III}(OH)/Rh^{II}}$ and $i_{\left[\mathrm{Rh^{II}}\right]_2/Rh^{I}}$ related to the reduction of (DPDE)Rh^{II} to (DPDE)Rh^{II}, (DPDE)Rh^{III} to (DPDE)Rh^{II}, (DPDE)Rh^{III}(OH) to (DPDE)Rh^{II} and [(DPDE)Rh^{II}]$_2$ to (DPDE)Rh^{I}, respectively. The resulting current follows BV equation involving the influence of rate constant taken to predict experiments,

$$\begin{aligned} i &= i_{Rh^{III}/Rh^{II}} + i_{Rh^{II}/Rh^{I}} + i_{Rh^{III}(OH)/Rh^{II}} + \\ &+ \left[- k^{3}_{red} \Gamma_{Rh^{III}(OH)} + k^{3}_{ox} \Gamma_{Rh^{II}} \right] + \left[- k^{4}_{red} \right. \end{aligned} \tag{14}$$

where the rate constants of BV model, k^{j}_{red} and k^{j}_{ox}, got have an exponential dependence with the applied potential which can be described as

$$k^{j}_{red} = k^{j}_{0} e^{-\alpha \frac{F}{RT}\left(E - E^{0}_{j}\right)} \tag{15}$$

$$k_{ox}^{\ j} = k_0^j e^{(1-\alpha)\frac{F}{RT}\left(E - E_j^0\right)}$$

Here, the standard potentials, ($E_{1,2,3}^{\ 0}$) along with the standard heterogeneous rate constants ($k^{1,2,3}_{\ 0}$) depict the IAP process, while (k_{2f}/k_{2b}) and electro-degradation parameters k_0^4 and E_4^0 are introduced to include the dimeric species.

Supplementary methods 2:

As mentioned in the original document, in chronoamperometery (CA) the current is proportional to the instant concentration of enzyme "active form". In this study, the transient states are given by the following equation connecting the active and inactive forms of the enzyme,

$$Rh^{III} \underset{k_A}{\overset{k_I}{\rightleftharpoons}} Rh^{III}(OH) \tag{1}$$

The expression for the fraction of the conversion of Rh^{III} is described in Equation 2. The function is expressed by the fraction of only active rhodium form (Rh^{III}) when applying a constant potential,

$$\frac{d\Phi_{Rh^{III}}}{dt} = -k_I \Phi_{Rh^{III}} + k_A\left(1 - \Phi_{Rh^{III}}\right) \tag{2}$$

The Equation 1.4 is obtained with the initial condition and boundary conditions,

$$\Phi_{Rh^{III}} = \left(\Phi^{*}_{Rh^{III}} - \frac{k_A}{k_I + k_A}\right) e^{-\left(k_I + k_A\right)t} + \frac{k_A}{k_I + k_A} \tag{3}$$

where $\Phi^{*}_{Rh^{III}} = \Phi_{Rh^{III}}$ at $t = 0$ is the starting fraction of the rhodium in active form. Meaningful parameters are introduced, in which $\Phi^{\infty}_{Rh^{III}}$ is the asymptotic value and $1/k_{tot}$ is the time constant of the exponential relaxation toward steady-state

$$\Phi^{\infty}_{Rh^{III}} = \frac{k_A}{k_I + k_A}$$
$$\frac{1}{k_{tot}} = \frac{1}{k_I + k_A} \tag{4}$$

In the transient-state kinetics, this is a typical treatment of relaxation experiments1,2. The total catalytic current equals the time-dependent fraction times the steady-state current behaviour of the active rhodium, $i^{lim}_{Rh^{III}}$, at a certain high driving force.

$$i = \Phi_{Rh^{III}}\, i^{lim}_{Rh^{III}} \tag{5}$$

The limiting current is given

$$i_{Rh^{III}}^{lim} = 2FA\Gamma^{*}k_{cat} \tag{6}$$

where A is the electrode surface area, Γ^{*} is the total surface total surface excess, and k_{cat} is the potential-dependent turnover rate of the completely active reactant. The total current is represented in Equation 7 by summation of Equations 2 to 6.

$$i = i_{Rh^{III}}^{lim}\left[\left(\Phi_{Rh^{III}}^{*} - \Phi_{Rh^{III}}^{\infty}\right)e^{-k_{tot}t} + \Phi_{Rh^{III}}^{\infty}\right] \tag{7}$$

We define $i_0 = i_{Rh^{III}}^{lim}\Phi_{Rh^{III}}^{*}$ and $i_\infty = i_{Rh^{III}}^{lim}\Phi_{Rh^{III}}^{\infty}$, and Equation 7 can be reorganised as

$$i = (i_0 - i_\infty)e^{-k_{tot}t} + i_\infty \tag{8}$$

Equation 8 implies that fitting an exponential relaxation to the chronoamperometric data provides the currents and k_{tot}, which can deduce the kinetics by combining the initial value of $\Phi_{Rh^{III}}$ and $\Phi_{Rh^{III}}^{*}$. k_I and k_A follow

$$\begin{aligned} k_A &= \Phi_{Rh^{III}}^{*}\frac{i_\infty}{i_0}k_{tot} \\ k_I &= k_{tot} - k_A \end{aligned} \tag{9}$$

Now when we apply a potential E_1 smaller than the standard potential E_0 from time t_1 to t_2, then an inactivation potential E_2 from time t_2 to t_3 and finally a reactivation potential E_3 after time t_3, the governing equations for the current are

$$i(t_1 < t < t_2) = i_{Rh^{III}}^{lim}(E_1)\left\{\left[1 - \Phi_{Rh^{III}}^{\infty}(E_1)\right]e^{-k_{tot}(t-t_1)} + \Phi_{Rh^{III}}^{\infty}(E_1)\right\} \tag{10}$$

$$i(t_2 < t < t_3) = i_{Rh^{III}}^{lim}(E_2)\left\{\left[\Phi_{Rh^{III}}^{'} - \Phi_{Rh^{III}}^{\infty}(E_2)\right]e^{-k_{tot}(t-t_2)} + \Phi_{Rh^{III}}^{\infty}(E_2)\right\} \tag{11}$$

$$i(t > t_3) = i_{Rh^{III}}^{lim}(E_3)\left\{\left[\Phi_{Rh^{III}}^{''} - \Phi_{Rh^{III}}^{\infty}(E_3)\right]e^{-k_{tot}(t-t_3)} + \Phi_{Rh^{III}}^{\infty}(E_3)\right\} \tag{12}$$

in Equation 10, the starting fraction as initial boundary assumes unity to give enough time to be active. From Equations 11 and 12, the starting fractions when stepping down the applied

potential are given as the results at the sweeping-potential time, and the value can be calculated as following,

$$\Phi_{Rh^{III}}^{'} = \left[1 - \Phi_{Rh^{III}}^{\infty}(E_1)\right] e^{-k_{tot}(t_2 - t_1)} + \Phi_{Rh^{III}}^{\infty}(E_1) \quad (13)$$

$$\Phi_{Rh^{III}}^{''} = \left[\Phi_{Rh^{III}}^{'} - \Phi_{Rh^{III}}^{\infty}(E_1)\right] e^{-k_{tot}(t_3 - t_2)} + \Phi_{Rh^{III}}^{\infty}(E_2) \quad (14)$$

Supplementary Figures

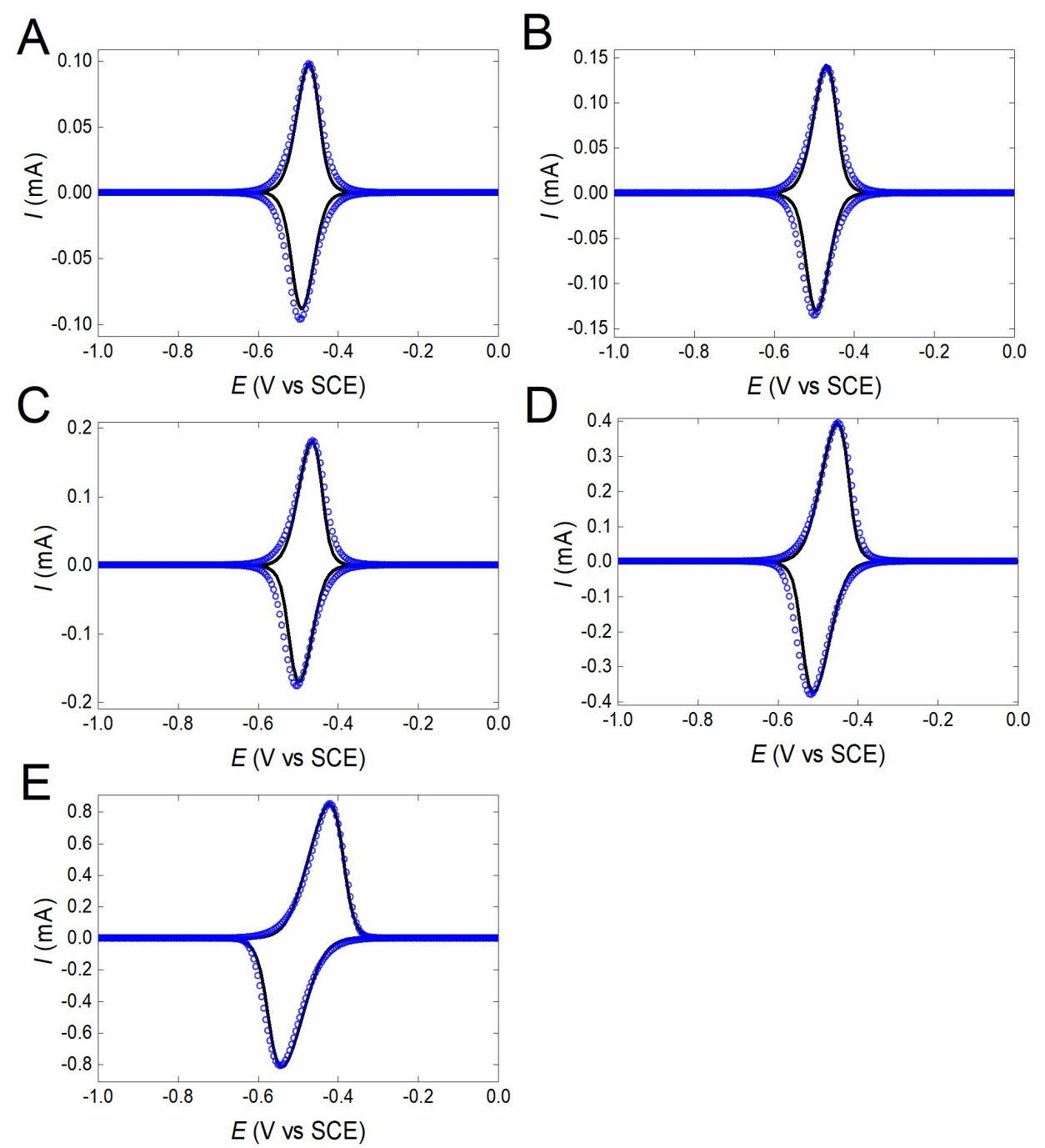

Supplementary Figure 1. Validation of the EC'CE model predictions, that lacks the formation of dimer, for non-catalytic system at different scan rates. The black solid line (⁻) represent the experiments and the blue circles (ᵒ) represent the model predictions at scan rates of (A) 50, (B) 75,

(C) 100, (D) 200 and (E) 500 mV/s. These validations are for the experimental data obtained in 0.1 M KOH

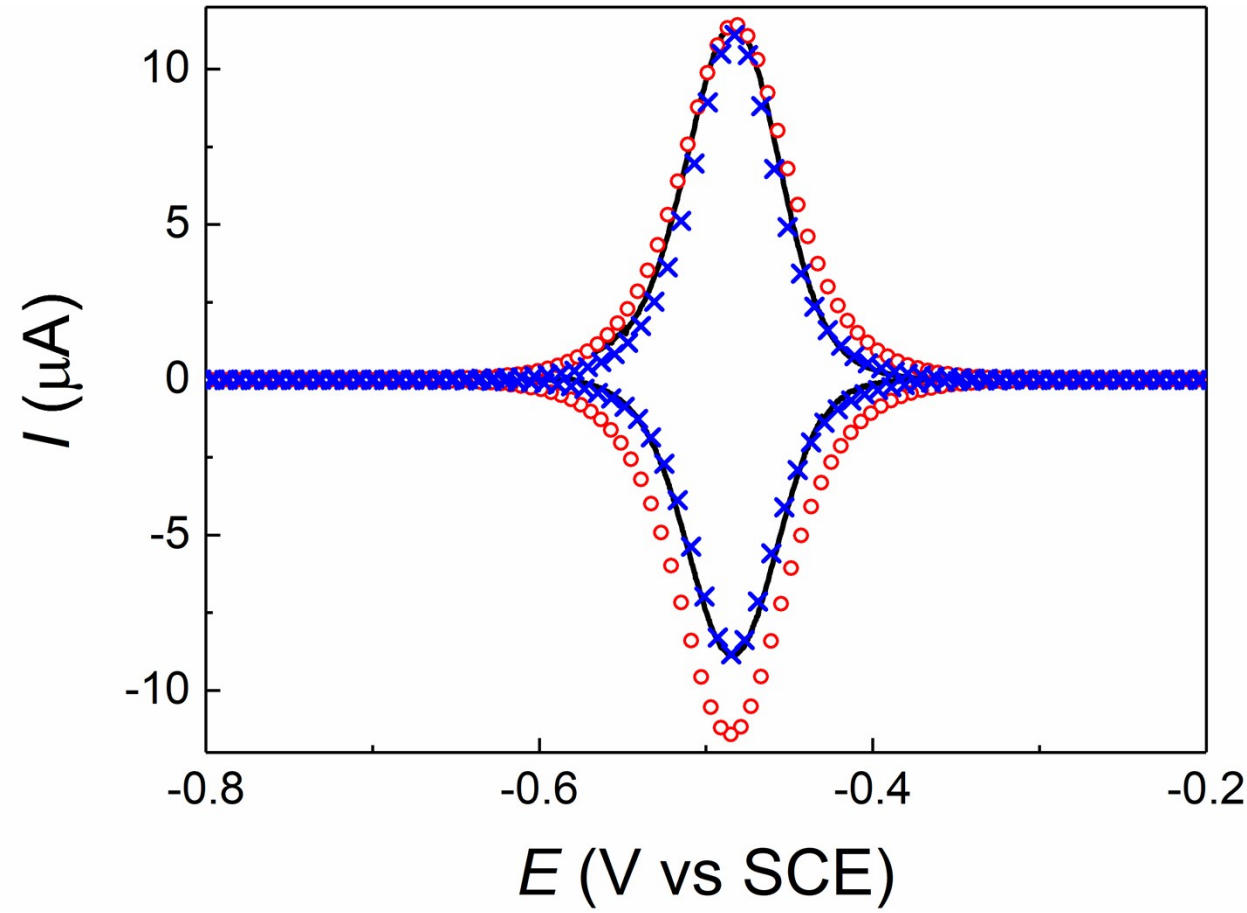

Supplementary Figure 2. Comparison of the two model predictions for non-catalytic system to the experimental data. The black solid line ($^{-}$) represent the experiments, the red circles (^{o}) represent the EC'CE model predictions and the blue crosses (^{x}) represent the EC'CECE model predictions at a scan rate of 5 mV/s in 0.1 M KOH.

References

1 Limoges, B. ı. & Savéant, J.-M. Catalysis by immobilized redox enzymes. Diagnosis of inactivation and reactivation effects through odd cyclic voltammetric responses. *Journal of Electroanalytical Chemistry* **562**, 43-52 (2004).

2 Pandelia, M.-E. *et al.* Membrane-bound hydrogenase I from the hyperthermophilic bacterium Aquifex aeolicus: enzyme activation, redox intermediates and oxygen tolerance. *Journal of the American Chemical Society* **132**, 6991-7004 (2010).